Automated Impedance Matching System for Robust Wireless Power Transfer via Magnetic Resonance Coupling

Teck Chuan Beh, *Student Member, IEEE*, Masaki Kato, *Non Member, IEEE*, Takehiro Imura, *Member, IEEE*, Sehoon Oh, *Member, IEEE*, Yoichi Hori, *Fellow, IEEE*

***Abstract*— Recently, a highly efficient mid-range wireless transfer technology using electromagnetic resonance coupling was proposed, and has received much attention due to its practical range and efficiency. The resonance frequency of the resonators changes as the gap between the resonators change. However, when this technology is applied in the MHz range, the usable frequency is bounded by the Industrial, Science, Medical (ISM) band. Therefore, to achieve maximum power transmission efficiency, the resonance frequency has to be fixed within the ISM band. In this paper, an automated Impedance Matching (IM) system is proposed to increase the efficiency by matching the resonance frequency of the resonator pair to that of the power source. The simulations and experiments verify that the IM circuits can change the resonance frequency to 13.56MHz (in the ISM Band) for different air gaps, improving the power transfer efficiency. Experiments also verified that automated IM can be easily achieved just by observing and minimizing the reflected wave at the transmitting side of the system.**

***Index Terms*—Automation, Impedance Matching, Maximum Efficiency, Resonance Frequency, Wireless Power Transfer,**

I. Introduction

NOWADAYS, with the development of mobile appliances and the recent boom of electric vehicles (EV), the need for a technique to wirelessly charge these appliances has increased[1][2]. A convenient, safe and efficient way to charge these devices can increase the mobility, reduce the cost and improve safety. As a result, the Wireless Power Transfer (WPT) field has enjoyed great progress. Recent researches include WPT for small electronic devices such as mobile appliances [3] [4] and medical implants[5]- [7], and bigger, high power devices such as electric vehicles (EV)[8][9].To make wireless charging more practical, the charging system has to be efficient, high power, and be able to transfer power through large air gaps. Currently, there is no such technology.

The most common WPT technology now is the electromagnetic induction method, which is a very efficient non-radiative WPT. However, it generally has a small air-gap at a few centimeters, and recently improved to approximately 10cm by increasing its frequency to 20-40kHz. Furthermore, its efficiency drops severely when there is misalignment between its transmitting and receiving coils, even when the misalignment is only several centimeters. While this technology is sufficient to charge most electric appliances, it might not be convenient enough to realize a charge-on-the-go system. Recently, a highly efficiency mid-range WPT technology using magnetic resonance coupling (MRC) was rediscovered and proposed [10]- [12], and has received much attention due to its high efficiency and practical mid-range [13]- [15]. It has an efficiency of approximately 90% within 1 meter, and 45% at 2 meters [10][11].

The resonance frequencies of the resonator pair change as the gap vary [16]- [19]. Therefore, a system to maintain resonance even at varying gap is needed to maintain the high efficiency. There are many methods to conduct this such as Impedance Matching (IM) [19][20], frequency matching [21], coupling manipulation[11][22] and changing the resonator parameters[23]. Studies show that the resonance can be maintained with these matching theories. However, to apply this technology in the MHz range, which allows smaller and more efficient resonator, the usable frequency range is bounded by the Industrial Scientific Medical (ISM) band. This means that a system to fix the resonance frequency of the resonators within the ISM band is also vital. Moreover, the matching system has to be automated to make a robust and practical system. In this case, frequency matching is not suitable as the resonance frequency often moves out of the ISM band. Manipulating the coupling in between the resonators and changing its parameters is also not practical as most practical systems has a fixed set of resonators that needs to adapt to different air gaps. On the other hand, IM not only satisfies the ISM condition, it also has no moving parts in its system, which

Manuscript received November 29, 2011; revised April 1, 2012 . Accepted for publication May 10, 2012. This research was conducted in the University of Tokyo.

T.C. Beh was with the Graduate School of Frontier Science, University of Tokyo, 227-8561, Chiba, Japan. He is now with GE Healthcare Japan, 191-8503, Tokyo, Japan. (e-mail: teckchuan.beh@ge.com).

M. Kato, T. Imura and Y.Hori are with the Graduate School of Frontier Science, University of Tokyo, 227-8561, Chiba, Japan. (e-mail: kato@hori.k.u-tokyo.ac.jp; imura@hori.k.u-tokyo.ac.jp; hori@k.u-tokyo.ac.jp).

S. Oh was with the Department of Electrical Engineering, University of Tokyo, Tokyo, Japan. He is now with Samsung Heavy Industries, Korea. (e-mail: sehoon74@gmail.com).

is generally considered desirable, especially in the automotive industry.

This paper studies the MRCWPT system which has a fixed frequency of 13.56MHz. The aim of this research is to fix the resonance frequency of the system within the ISM band, and increase its efficiency by introducing an automated IM system. To do so, in this paper, we verified the effects of IM [19][20] and tested the viability of an automated system through simulations and experiments.

II. Magnetic Resonance Coupling (MRC)

The magnetic resonant coupling phenomenon has been explained in detail using the mode coupling method [10][11]. However, this theory is often complicated and inconvenient when it comes to designing the circuits around the resonators. To overcome this problem, a design and analysis method using an equivalent circuit based on resonator and circuit design theories was proposed in papers [15]– [18]. These papers show that the experimental results match the electromagnetic analysis and circuit simulations. Using the equivalent circuit, the frequency characteristics of the resonators can be estimated up to an accuracy of 5% error. [17] In this paper, the characteristics of the resonators are analyzed based on the equivalent circuits and experiments. Fig. 1 shows the resonator prototype we created to conduct WPT via MRC.

Fig. 1. Wireless power transfer using prototype resonators used in the experiments.

TABLE I
Parameters of Resonators

Self resonance frequency	13.56MHz
Antenna type	Open, Spiral
Number of turns	5 turns
Radius	15cm
Pitch	5mm
Outer diameter of coil	2mm
Inductance (L)	10300nH
Capacitance (C)	13.26pF
Ohm Resistance (R)	1.5Ω
Q value (at 13.56MHz)	590

A. Equivalent Circuit of MRC

Wireless power transfer through MRC involves creating an LC resonance, and transferring the power through magnetic coupling without radiating electromagnetic waves. Hence, the magnetic coupling can be represented as mutual inductance L_m as in Fig. 2. TABLE I shows the design of the resonators as well as the LC parameters of the resonators as measured by the vector network analyzer (VNA). The Q value is defined as ratio of the reactance generated by the calculated inductance L, and the real part of the impedance measured by the VNA at the resonance frequency (13.56MHz). The equivalent circuit for the resonator parameters depends on the antenna design. [17]The resonator studied in this paper is an open spiral antenna, where it is made of two layers of spiral coils, each 2.5 loops each. Although this resonator does not include a capacitor, the characteristics of the open ended coil and the pitch in between the two coil layers make up for the capacitance. Hence, along with the inductance from the length of the coils, the resonator is represented as series set of lumped inductor L and capacitor C.[18]

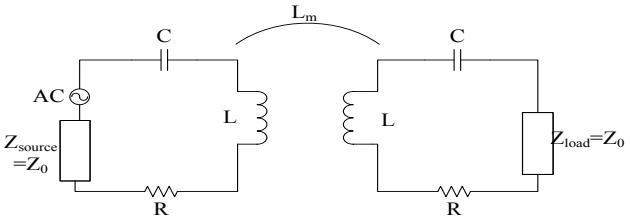

Fig. 2. Equivalent circuit of wireless power transfer system via magnetic resonance coupling without tuning circuit.

Z_{source} in Fig. 2 represents the characteristic impedance of the source, and Z_{load} is the impedance of the load. In this paper, they are both set to be Z_0, 50Ω the default characteristics of most high frequency system. R represents the ohm loss and radiation loss of the resonators.

The resonance frequency of the resonator pair can be calculated based on the equivalent circuit. To satisfy the resonance condition, the reactance of Fig.2 must be zero, equation (1). This can be satisfied by two angular resonance frequencies as shown in equation (2) and (3).The subscripts "*m*" and "*e*" in these two equations represents the two angular resonance frequencies where the magnetic and electric wall is formed at the plane of symmetry respectively. The magnetic field in the former is strong at the center of the coils, while the latter has strong magnetic fields at the edge of the coils. Both these frequencies allows high efficiency wireless power transfer through magnetic resonance coupling[24] The coupling coefficient k can be derived from equation (2) and (3) into equation (4).

$$\frac{1}{\omega L_m}+\frac{2}{\omega(L-L_m)-\frac{1}{\omega C}}=0 \tag{1}$$

$$\omega_m=\frac{\omega_0}{\sqrt{(1+k)}}=\frac{1}{\sqrt{(L+L_m)C}} \tag{2}$$

$$\omega_e=\frac{\omega_0}{\sqrt{(1-k)}}=\frac{1}{\sqrt{(L-L_m)C}} \tag{3}$$

$$k=\frac{L_m}{L}=\frac{\omega_e^2-\omega_m^2}{\omega_e^2+\omega_m^2} \tag{4}$$

Next, the efficiency of the power transfer is calculated based on the equivalent circuit. The power reflection ratio η_{11} and transmission ratio η_{21} is defined in equation (5) and (6) where S_{11} and S_{21} represent the wave reflection and transmission ratio respectively. For simplification purposes, R is considered to be 0Ω, and S_{21} can be calculated from equation (7) [16].

$$\eta_{11}=|S_{11}|^2\times 100[\%] \tag{5}$$

$$\eta_{21}=|S_{21}|^2\times 100[\%] \tag{6}$$

$$S_{21}(\omega)=\frac{2jL_mZ_0\omega}{L_m^2\omega^2+\left[(Z_0+R)+j(\omega L-\frac{1}{\omega C})\right]^2} \quad (7)$$

B. Frequency Characteristics of MRC

As the gap in between the resonators change, the coupling coefficient *k* between the resonators will also vary. This causes a change in the impedance of the system, which leads to a change in resonance frequency and the power transfer efficiency.

Fig. 3 shows the frequency characteristics of the power reflectionη_{11} and transmission ratio $\eta_{21}$of the system as measured by a vector network analyzer and calculated using equation (5) and (6). The gap *g* between the resonators was varied from 6cm to 31cm. As shown in the figure, when the gaps are small and the coupling is strong, there exist two resonance frequencies that achieve maximum power transfer efficiency. As the gap becomes larger, the resonance frequencies moves closer to each other and eventually merges into one. Then, if the gap gets even larger, the maximum efficiency will drop.

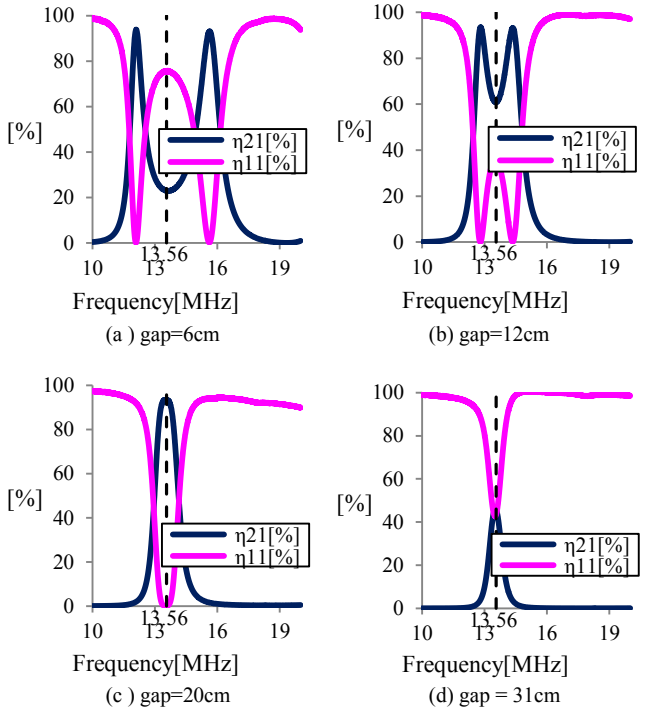

Fig. 3. Experimental results of efficiency versus frequency at different air gap.[17]

III. Proposed WPT System with Impedance Matching

The frequency characteristic in Fig. 3 shows that there is a need to match the resonance frequency of the resonators to the frequency of the power source to create a highly efficient WPT system that is robust to positional displacements. In this paper, an automated IM system is proposed to achieve that goal. This section goes through the basic theory of IM, and explains the setup of the proposed IM system.

A. Basic Theory of Impedance Matching

IM is a technique commonly used in the power transfer and communication industry to improve the efficiency of the system. It is usually done by inserting a matching network such as an LC circuit to minimize the wave reflection ratio. Fig. 4 represents a simple circuit with an AC source. The characteristic impedance of the source is defined as Z_{source}, and the load impedance is defined as Z_{load}. The power transferred to the load can be written as equation (8), and it reaches its maximum when Z_{source} is the conjugate of Z_{load} ($Z_{source}=Z^*_{load}$) to make equation (9). In other words, the circuit is matched and its efficiency maximized when the impedance of the load from the source's point of view matches the conjugate of Z_{source}, vice versa.

$$P_{load}=I^2Z_{load}=\frac{V^2}{Z_{source}}\left(\frac{1}{\frac{Z_{source}}{Z_{load}}+2+\frac{Z_{load}}{Z_{source}}}\right) \quad (8)$$

$$P_{\max}=\frac{V^2}{4Z_{source}} \quad (9)$$

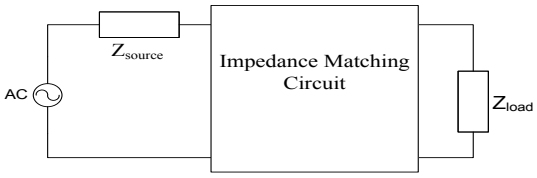

Fig. 4. Equivalent circuit explaining the common structure of IM system.

The IM circuit can be considered a two-port network that is described in equation (10). The matching conditions are satisfied when the parameters satisfy equations (11) and (12).

$$\begin{pmatrix}V_1\\I_1\end{pmatrix}=\begin{pmatrix}A & B\\C & D\end{pmatrix}\begin{pmatrix}V_2\\I_2\end{pmatrix} \quad (10)$$

$$Z_{source}=\sqrt{\frac{AB}{CD}} \quad (11)$$

$$Z_{load}=\sqrt{\frac{DB}{CA}} \quad (12)$$

B. Setup of Proposed IM system

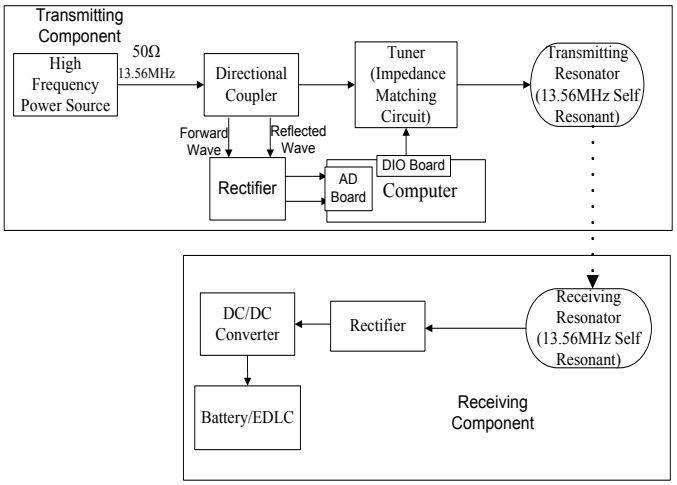

Fig. 5.Proposed WPT system with automated IM.

Based on the theory explained above, an automated IM system is designed to match the resonators in the MRC based WPT system. Fig. 5 shows the diagram of the proposed automated IM system. The system transfers the power from the 13.56MHz power source to the load through the two resonators with identical self-resonance frequency. The power is transferred through MRC between the resonators, and it is rectified to charge energy storage mediums such as batteries. The characteristic impedance of the power source and the BNC cables are 50Ω in this paper. Under normal circumstances, the coupling coefficient k (affected by the gap) between the resonator, and the impedance of the load (50Ω in this paper) is unknown and variable. Only the voltage, current and wave reflection ratio can be measured in the transmitting side of the system.

In the proposed system, a directional coupler is inserted between the power source and the transmitting resonator to measure $S_{11,}$ the ratio of power that is reflected from the resonators back to the power source. The measured values are input into a computer which is used to control the parameters of the IM circuit. The main advantage of using the directional coupler is that the sensor is only needed at the transmitting side of the system, which usually has less space restrictions in practical cases. This also means that communication between the transmitting and receiving side of the system is not required, making it a cheap and simple system.

By minimizing theS_{11}, the proposed IM system will match the resonators, thus increasing the efficiency and range. Automating this system will allow the WPT to be robust towards positional displacements and changes in load impedance.

IV. Experimental Setup

This section explains the experimental setups used to verify the viability of the proposed system. Two experiments were conducted. *Experiment I* is conducted to test the effects of IM on the MRC based WPT system. *Experiment II* is conducted to test the viability of automation of the proposed IM system that is based on only input from the reflection wave at the transmitting side of the WPT system (Fig. 5). The results will be shown in the following section V.

There are several types of matching networks such as the L-match and Pi-match networks. Both matching networks can match the impedance of the system and reduce the reflection. The L-match networks are simpler, and the Pi-match networks have a greater degree of design freedom such as selecting the Q-value of the system. To study the requirements of IM circuit needed to maintain the efficiency, the simpler L-match network is used in this paper. Therefore, if the L-match network is sufficient to maintain the high efficiency, the Pi-match should theoretically be able to achieve it too, allowing more design freedom in future prototypes. Moreover, the L-match networks also require fewer components. As a result, it has the advantage of needing less space and having less stray reactance.

A. Experiment I: Verifying the Effect of IM on MRC

To confirm the effect of IM on the MRC wireless power transfer system, an L-type matching circuit was inserted between the transmitting resonator and the power source as in Fig. 6.The experiment was done using a VNA to measure the wave transmission ratio $S_{21}$and reflection ratio S_{11}, and selecting matching parameters that minimizes S_{11}. The IM circuit was made using air core coils and ceramic condensers to make the matching parameters required to match the resonators at 13.56MHz.

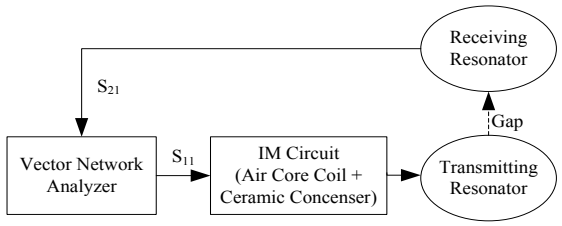

Fig. 6.Experimental setup to verify the effect of IM circuit.

Fig. 7 represents the equivalent circuits of the WPT system when an IM circuit is included. It is modified from Fig. 2 by inserting a two port IM circuit before the transmitting resonator, and converting it into a T-type equivalent circuit. Two types of L matching circuit topography were tested, namely the L-type matching circuit (Fig. 7(a)) and the inverted L-type matching circuit (Fig. 7(b)). The L-type matching circuit is used to match systems where the air gap is small and the overall impedance of the system is high. Likewise, when the overall impedance of the system is low due to a larger air gap, the inverted L-type matching circuit is used instead. These experiments were repeated for air gaps between the resonators at 6cm to 43cm to verify the effect of IM.

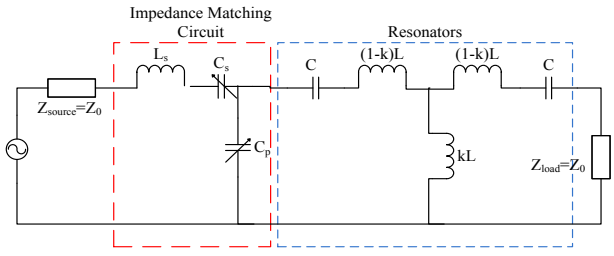

(a) L-type matching circuit

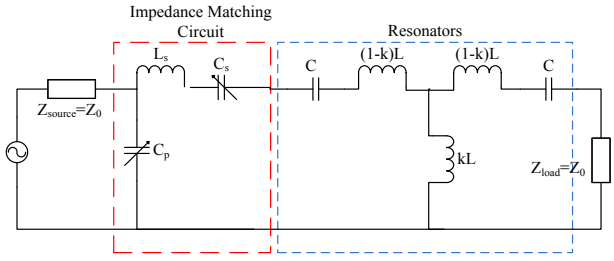

(b) Inverted L-type matching circuit

Fig. 7.Equivalent circuits of experimental setup of *Experiment I*,to verify the effect of IM circuit.

B. Experiment II: Verifying the Viability of Automation of Proposed IM System

While *Experiment I* tests the effect of IM on the WPT system, it does not prove that the proposed system in Fig. 5 can be automated to make it robust towards positional displacements. To do so, a prototype of the proposed WPT system was created for *Experiment II*. Fig. 8 shows the photo of the IM circuit used in the experimental setup, and Fig. 9 is the equivalent circuit of the system including the IM circuit.

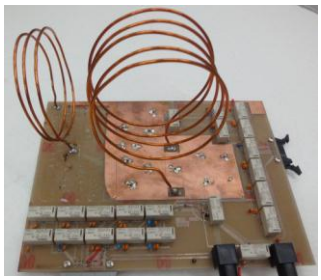

Fig. 8.IM circuit used in the automation experiment. Multiple high frequency relays are used to select the ceramic condensers and coils used for matching.

The IM circuit was made using a print circuit board, ceramic capacitors, air core coil, and high frequency reed relays. The relays act as switches to select the matching parameters, and are controlled using the computer through the digital input-output (DIO) board. The layout was set such that both the L-type and inverted L-type matching circuit can be realized. The IM circuit can also be bypassed (Thru). The advantages of using relays combined with ceramic condensers and air core coils is that they have the least loss (due to a high Q value), and that they have extremely quick switching speed (which allows a fast matching speed). The physical limit of the matching speed will only be determined by the chattering of the reed relays (5ms in this paper) as the high frequency used leads to an extremely fast response. For high power situations, the ceramic capacitors can be replaced with high Q components such as vacuum capacitors. In these experiments, the sampling time is 1ms, and the value of S_{11} is calculated from the average of five samples.

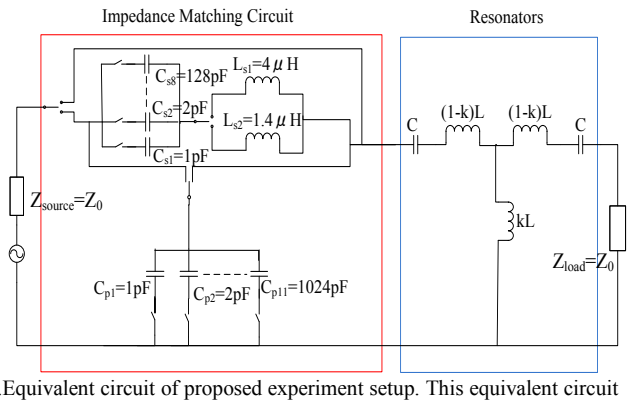

Fig. 9.Equivalent circuit of proposed experiment setup. This equivalent circuit is the extension of the equivalent circuit in Fig. 7, where relays act as switches to choose the required matching topography and matching parameters.

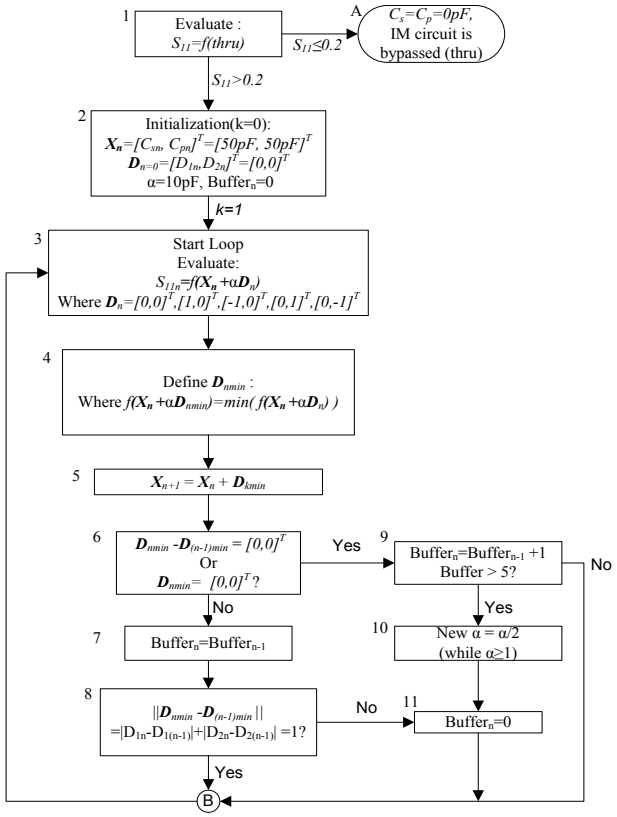

Fig. 10 Flow chart of the matching algorithm used in the experiment. The search algorithm is based on the best-step steepest descent search with scaling. It consists of three main parts, namely the Initialization (1,2), Search Loop (3 to 5), and Scaling Calculation (6 to 11)

Search Algorithm Used in Experiment II

The parameters of the IM circuit have to be tuned so that the S_{11} measured by the directional coupler reaches its minimum (ideally zero) for resonance to occur. As the objective of the experiment was to verify the possibility of automation in the system, a simple matching algorithm was selected in this particular experiment. In this paper, the best-step steepest descent search is used to show both the viability and simplicity of the automation of the IM system.

Fig. 10 shows the flow of the matching algorithm used in the experiment. The process is split into three parts. The initialization (1,2), search loop (3 to 5), and scaling calculation (6 to 11). It goes as in the following process:

1. The IM circuit is bypassed (thru), and the S_{11} is measured. If the S_{11} is sufficiently small (<0.2), the IM circuit will remain bypassed (A) as the resonators are already resonating.
2. If S_{11} is bigger than 0.2, the optimization algorithm is initialized before starting the search loop. *n* represents the loop count of the optimization process. The matching parameters, $\boldsymbol{X}_n=[C_{sn},C_{pn}]^T$is initialized at $[50pF,50pF]^T$. The vector of the direction of the step used to find the steepest descent $\boldsymbol{D}_n$, size of the step α_n, buffer count used in the step size scaling Buf_n, are initialized at $[0,0]^T$, 10pF, and 0 respectively.
3. When the matching parameters are inserted, S_{11}can be represented as a function of $\boldsymbol{X}_n$. In this step, the $S_{11}$for

($\boldsymbol{X}_n + \alpha_n \boldsymbol{D}_n$), where $\boldsymbol{D}_n$ is $[0,0]^T$,$[1,0]^T$,$[-1,0]^T$,$[0,1]^T$,$[0,-1]^T$, is evaluated.

4. The direction with the lowest S_{11} from the five directions mentioned in step 3, $\boldsymbol{D}_{nmin}$ is evaluated.
5. The step which produces the lowest S_{11}, ($\boldsymbol{X}_n + \alpha \boldsymbol{D}_{nmin}$) is chosen as the next matching parameter $\boldsymbol{X}_{n+1}$. The portion of the search algorithm that involves changing the marching parameters ends here.

6 to 11.From step 6 to step 11, a calculation loop is inserted to determine the size of the next step α_{n+1}. There are four possible outcomes from this loop, which are

(a) Path I: (6→7→8→B).
The buffer count Buf_n and step size α_{k+1} of the next loop will remain as it is if the $\boldsymbol{D}_{nmin}$ is not $[0,0]^T$ and $\boldsymbol{D}_{(n-1)min}$ is $[0,0]^T$.

(b) Path II: (6→7→8→11→B).
The next step size α_{n+1} will remain the same but the buffer count Buf_n reinitialized to 0 if $\boldsymbol{D}_{nmin}$and$\boldsymbol{D}_{(n-1)min}$ is not $[0,0]^T$, and not in the opposite direction of each other.

(c) Path III: (6→9→B).
If $\boldsymbol{D}_{nmin}$ is $[0,0]^T$ or the opposite direction of $\boldsymbol{D}_{(n-1)min}$, the buffer count Buf_n increases by 1 while the step size remains the same.

(d) Path IV: (6→9→10→11→B).
If the conditions in 6(c) are satisfied and Buf_k is larger than the buffer limit (set at 5), $Buf_n$is reset to 0 and the size of the next step (α_{n+1}) is scaled to half the present size (α_n). This scaling is repeated untilα is 1pF to get a higher precision in matching.

B) Once $\boldsymbol{X}_{n+1}$and α_{n+1} are determined, the loop returns to step 3 with the newly determined parameters.

V. Simulation and Experimental Results

Section IV explained in detail the experimental setups and methods used in this paper. This section shows the experimental and simulation results of thetwo studies in this paper. Part A shows the experimental results of *Experiment I*, which is conducted to verify the effect of IM. Next, Part B shows the simulation results on the characteristics of S_{21} of the WPT system when the matching parameters (C_s, C_p) are varied. Finally, Part C is the experimental results of *Experiment II*, which is conducted to prove the viability of automation in the proposed IM system.

A. Experiment I Results: Effect of IM on MRC

Fig. 11 shows the simulation conducted with LT-Spice on the equivalent circuit Fig. 7(a) and (b). The graphs show the frequency characteristics of the power transmission $\eta_{21}$and reflection ratio η_{11}. The efficiency of the system is defined as η_{21}, and it reaches maximum when resonance occurs (η_{11}becomes zero). The results show that the L-type IM circuit (Fig. 11(a)) can be used to when frequency splitting occurs to shift the resonance frequency to the frequency of the power source, thus increasing the efficiency. On the other hand, the inverted L-type IM circuit (Fig. 11(b)) improves the efficiency by creating a sharper peak at the resonance frequency. These simulation results are verified by the experiment in Fig. 12. 5% of the loss is due to the radiation and ohm loss of the resonators, and the next 5-15% decrease in efficiency in the experimental results is mainly due to the ohmic loss of the components and copper wires used to make the IM circuit.

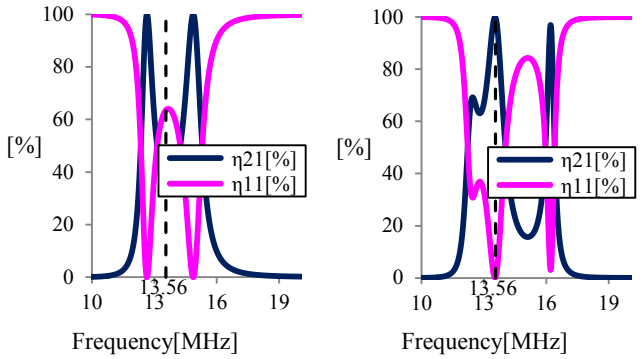

(i) Before matching (ii)After matching

(a) L matching circuit (k=0.17, L_s=6μH,C_s=32pF,C_p=78pF)

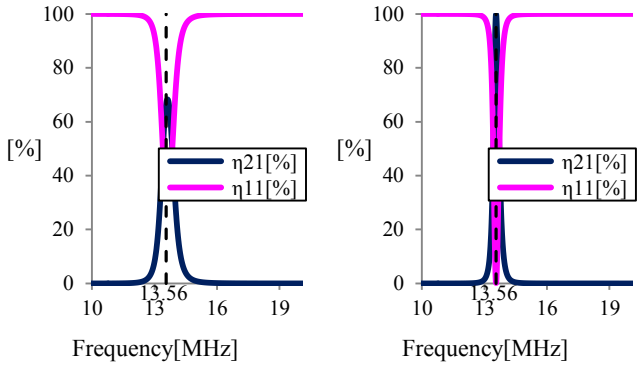

(i) Before matching (ii)After matching

(b) Inverted L matching circuit (k=0.03, L_s=6μH,C_s=24pF,C_p=385pF)

Fig. 11.Simulation results.Frequency characteristics of the system before and after matching. This simulation is based on the equivalent circuits in Fig. 7. The Ohm Loss of the copper wires of the antennas R, is considered zero in this simulation.

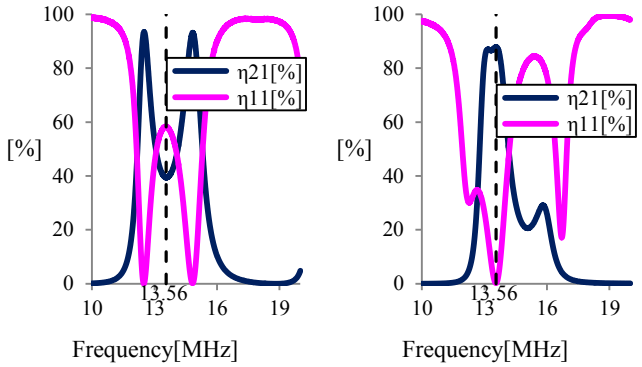

(i) Before matching (ii)After matching

(a) Gap=9cm, (d/D=0.3) (L_s=3.66μH,C_s=51pF,C_p=35pF)

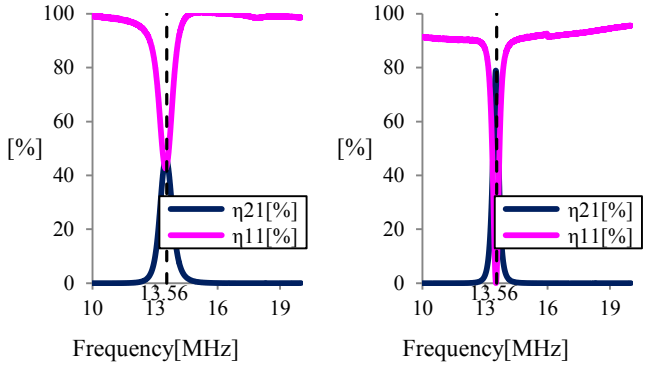

(i) Before matching (ii)After matching

(b) Gap=31cm, (d/D=1.03) (L_s=1.43μH,C_s=102pF,C_p=440pF)

Fig. 12.Experimental results. Frequency characteristics of the system before and after matching. L-matching circuit is used for Gap=9cm and Inversed L-matching is used for 31cm. The *d*/*D* in the first bracket represents the distance/diameter, which is the normalized value of the gap to the diameter of the resonator. The parameters in the second bracket is describes the IM parameters after matching is conducted.

B. Simulation on Characteristics of S_{21} versus Matching Parameters (C_s,C_p)

We have verified that the efficiency of the resonators can be improved using an IM circuit. Before automation can be done, it is vital to know how the transmission and reflection ratio changes as the matching parameters change so that a suitable matching algorithm and hardware design can be chosen. For example, in the event that local peaks exists, a more sophisticated matching algorithm such as particle swarm optimization will need to be implemented instead of simple two dimensional optimization algorithms such as the steepest gradient method. The sharpness of the peak will also determine the precision of the tuning parameters and optimization algorithm required. Therefore, a simulation was conducted using MATLAB to study the characteristics of S_{21} as capacitance used to set the matching parameters (C_s, C_p) change.

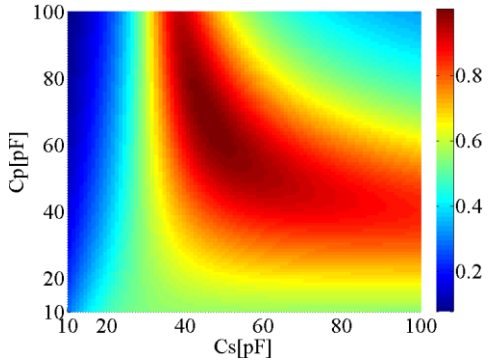

(a) k=0.2(small gap)

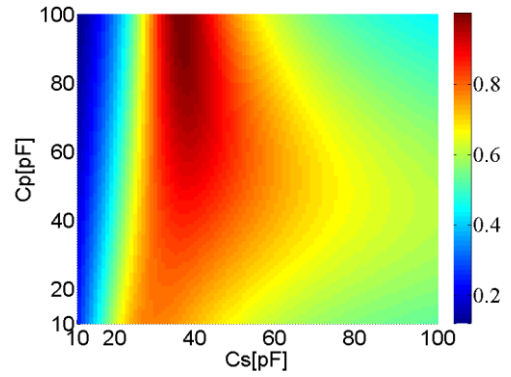

(b) k=0.12(medium gap)

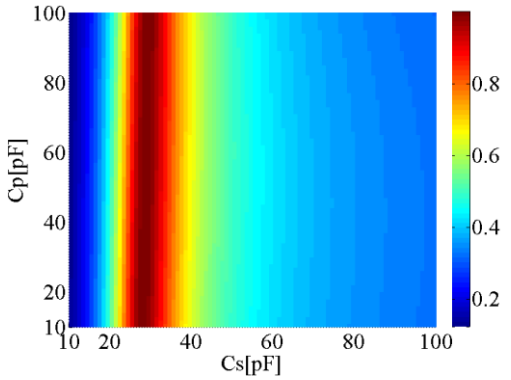

(c) k=0.06(large gap)

Fig. 13.Simulation results.S_{21} ofthe resonators when C_s and C_p are varied. L_s=5μH in this simulation.

Fig. 13 shows the simulation results of S_{21} in the equivalent circuit in Fig. 7(a) when the matching parameters (C_s, C_p) are varied from 10pF to 100pF.The inductor L_s used in the matching circuit is set to be 5000nH, and the coupling coefficient *k* is varied from 0.05 (large gap) to 0.25 (small gap). Based on the figure, we can observe that there is only a single peak with relatively gentle slopes at strong couplings and steeper slopes at weaker coupling. This means that almost any optimizing algorithm can be used to tune the system as long as the precision of the tuning parameters are sufficiently high. In this case, 1-2pF for C_s and 5pF for C_p will be sufficient to tune the system. Another issue that has to be dealt with is the parts where the gradient are too slight as the change in signal to noise ratio of the directional coupler as the parameters change becomes too small. One way to deal with this issue is by measuring the S_{11} from parameters further apart so that the S_{11} signal difference of will be larger.

C. Experiment II Results: Viability of Automation of Proposed IM System

The results above verified the effect of IM on MRC, and showed that the parameter needed to match the resonators to maximum efficiency has only one global peak, with no local peaks. To make the WPT system robust towards positional displacements, an automated IM system is proposed. This section shows the results of the experiments conducted to test the viability of automation for the proposed system. These experiments were conducted at gaps 6cm to 30cm. For gaps

6cm to 20cm, the L-type IM network is used with L_s of approximately 4μH. The inversed L-type IM network is used with L_s of 1.4μH for gaps 21cm to 30cm. The automation experiment is conducted at approximately 8W from the power source, and the efficiency before and after the matching is measured with the VNA. The efficiency of the system is not affected by the input power according to [18] (from mW to 100W) as long as the resonator coils are not overloaded.

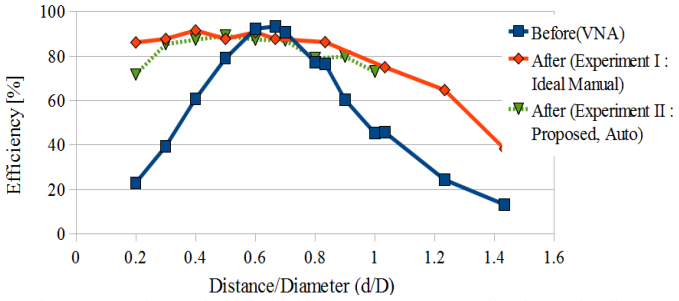

Fig. 14.Experimental results. Efficiency versus normalized transfer distance (gap) to the resonator diameter (Efficiency vs Distance/Diameter) graph of WPT using proposed automated impedance matching system. In this experiment, the diameter of the resonators is 30cm. Here, L-type IM network is used for gaps 6cm to 20cm, and the Inversed L-type IM network is used for gaps 21cm to 43cm.
Before(VNA) represents the efficiency (at 13.56MHz) of the resonators without the IM circuit. *After (Experiment I: Ideal, Manual)* represents the efficiency (at 13.56MHz) of the system after it is manually matched using the method and circuit introduced in *Experiment I*(Section IV.A). *After (Experiment II: Proposed, Auto)* is the efficiency (at 13.56MHz) of the system after it is automatically matched using the system proposed in Section IV.B.

Fig. 14 shows the efficiency versus gap graph of the experimental results. *After(Experiment I: Ideal, Manual)* can be considered the maximum efficiency that can be achieved as the size of the circuit is minimized, reducing all possible losses through ohm loss and stray reactance. The results show that the efficiency of the proposed IM circuit (*Experiment II*) can reach 85%, only 5% lower than the ideal case (*Experiment I*).The 5% loss is mainly due to the ohm loss caused by the bigger size of the automated IM circuit used in *Experiment II*. Moreover, by increasing the efficiency of the system, the IM circuit also increased the range where energy can be transmitted at maximum efficiency.

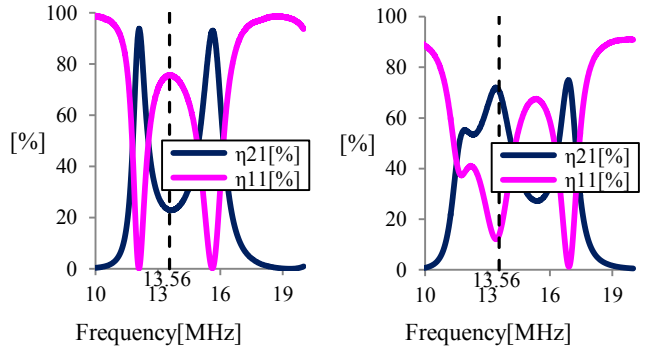

(i) Before matching (ii)After matching
(a) Gap=6cm,(d/D=0.2) (L-type, L_s=4μH,C_s=160pF,C_p=13pF)

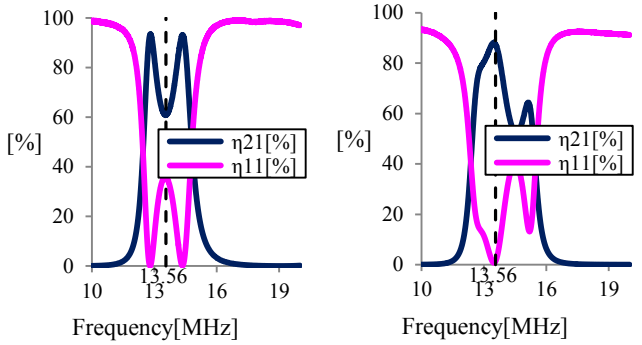

(i) Before matching (ii)After matching
(b) Gap=12cm, (d/D=0.4) (L-type, L_s=4μH,C_s=76pF,C_p=81pF)

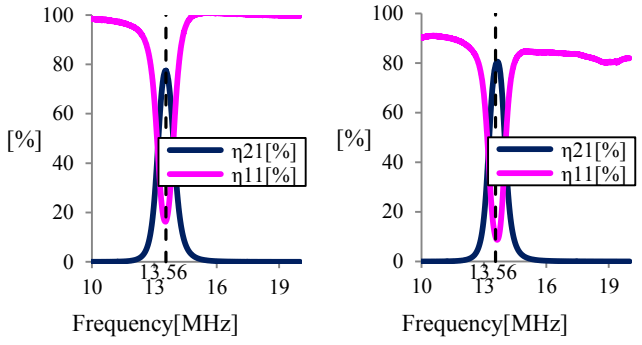

(i) Before matching (ii)After matching
(c) Gap=24cm, (d/D=0.8) (IM circuit bypassed)

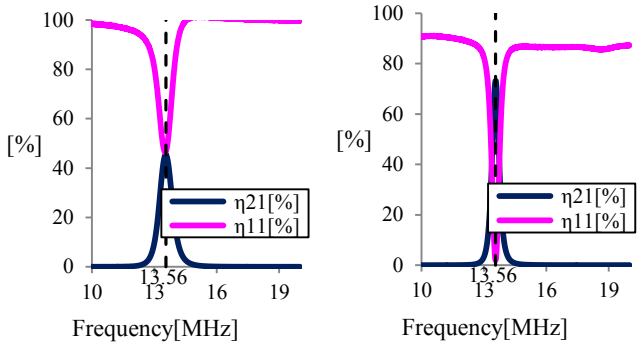

(i) Before matching (ii)After matching
(d) Gap=30cm, (d/D=1.0) (Inversed L, L_s=1.4μH,C_s=80pF,C_p=95pF)

Fig. 15. Experimental results of WPT with proposed automated IM system. Frequency characteristics before and after matching. L-matching circuit is used for gap=6cm and 12cm, while inversed L-matching is used for gap=30cm. The *d/D* in the first bracket represents the distance/diameter, which is the normalized value of the gap to the diameter of the resonator. The parameters in the second bracket is describes the IM parameters after matching is conducted. (Note: the results for (a)(i), (b)(i), (c)(i), (d)(i) are the frequency characteristics of the resonators when the IM circuit is not inserted)

Fig. 15 shows the frequency characteristics of the system before and after the automated matching is conducted. Fig. 15(b) and (d) shows the typical response of the experiments on L-type and inverted L-type matching network respectively, while Fig. 15(c) shows the results when the IM circuit is bypassed. The results in Fig. 15 verify that efficiency is increased by matching the resonators as in section III.B. This can be confirmed by noting that the S_{11} at 13.56MHz is very low, almost zero is most cases (Fig. 15(b) and (d)). As the IM circuit is bypassed in 24cm, the frequency characteristic does not significantly change as in Fig. 15(c). The 5% increase in

efficiency at Fig. 15(c) is not due to the matching process, but the change in frequency characteristics when the IM circuit is inserted before the transmitting resonator. The reason the S_{11} in Fig. 15(a)(ii) and (c)(ii) will be explained in the observation below.

Fig. 16 is the graph of the S_{11} versus the time as the experiment is conducted for gap 6cm, 12cm, 24cm and 30cm. The systems generally takes 0.25s to 1s to reach a wave reflection ratio of less than 10% and it takes up to 1.5s to completely settle. The results show that the simple algorithm tested can decrease the S_{11} to less than 10%, meaning the reflected power η_{11} is reduced to less than 1% (from equation (5)).This means that all the resonators were successfully matched. While the S_{11} for most experiments ended at almost 0%, the experiments for 6cm and 24cm show a final of approximately 8%. The S_{11} for 24cm stop at 8% because the IM circuit is bypassed as the reflection ratio is evaluated to be sufficient low. On the other hand, the result in the 6cm experiment could be due to the error in the S_{11} sensor reading caused by the non-linearity and the cutoff voltage of the diode used to rectify the AC signal from the directional coupler. (Note that the S_{11} reading at the computer's AD board is slightly different from that of the directional coupler due to the non-linearity and cutoff voltage of the diode.) This problem can be solved by improving the analog circuit used as the rectifier for the AD input, and enhancing the search algorithm.

Even with a simple matching algorithm that is not optimized for speed, the matching time is still significantly higher than regular IM systems that use variable condensers that are controlled by motors due to the fast switching speeds of the relays and the fast response of the 13.56MHz system. The matching speed is an important factor when dealing with moving objects and changing loads. To cope with these fast changing impedances, a more sophisticated matching control need to be applied. The options include improving the optimization search algorithm [25]- [28], and measuring the voltage and current at the transmission resonator to calculate the impedance so that a better set of initial parameters can be chosen.

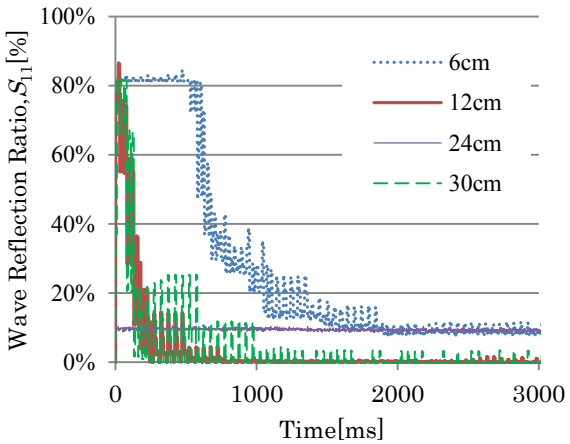

Fig. 16.Experimental results.S_{11}versus Time graph of automated impedance matching.

VI. Conclusion

As a conclusion, an automated IM circuit has been created to test its effects in maintaining resonance in a MRC wireless power transfer system with a fixed frequency (13.56MHz). The IM system uses a directional coupler to measure the reflected wave ratio at the transmitting end of the system, and high frequency relays to select the matching parameters needed to minimize the reflected wave.

Experiment results show that the proposed system increases the efficiency and extends the range of the wireless power transfer system. The efficiency increases to up to 85% (almost ideal) within 0.5s to 1.5s using a simple best-step steepest descent method search algorithm. The results also verified the validity of the automation of the IM system. It shows that automation can be easily achieved to make the system more robust towards changes in the gap and displacement of the receiving resonator.

References

[1] Zhen Ning Low; Chinga, R.A.; Tseng, R.; Jenshan Lin; , "Design and Test of a High-Power High-Efficiency Loosely Coupled Planar Wireless Power Transfer System," *Industrial Electronics, IEEE Transactions on* , vol.56, no.5, pp.1801-1812, May 2009.

[2] Hirai, J.; Tae-Woong Kim; Kawamura, A.; , "Study on intelligent battery charging using inductive transmission of power and information," *Power Electronics, IEEE Transactions on* , vol.15, no.2, pp.335-345, Mar 2000

[3] Chang-Gyun Kim; Dong-Hyun Seo; Jung-Sik You; Jong-Hu Park; Cho, B.H.; , "Design of a contactless battery charger for cellular phone," *Industrial Electronics, IEEE Transactions on* , vol.48, no.6, pp.1238-1247, Dec 2001

[4] Jabbar, H.; Song, Y.S.; Jeong, T.T.; , "RF energy harvesting system and circuits for charging of mobile devices," *Consumer Electronics, IEEE Transactions on* , vol.56, no.1, pp.247-253, February 2010

[5] Sai Chun Tang; Jolesz, F.A.; Clement, G.T.; , "A wireless batteryless deep-seated implantable ultrasonic pulser-receiver powered by magnetic coupling," *Ultrasonics, Ferroelectrics and Frequency Control, IEEE Transactions on* , vol.58, no.6, pp.1211-1221, June 2011

[6] Shiba, K.; Morimasa, A.; Hirano, H.; , "Design and Development of Low-Loss Transformer for Powering Small Implantable Medical Devices," *Biomedical Circuits and Systems, IEEE Transactions on* , vol.4, no.2, pp.77-85, April 2010

[7] Fei Zhang; Xiaoyu Liu; Hackworth, S.A.; Sclabassi, R.J.; Mingui Sun; , "In vitro and in vivo studies on wireless powering of medical sensors and implantable devices," *Life Science Systems and Applications Workshop, 2009. LiSSA 2009. IEEE/NIH* , vol., no., pp.84-87, 9-10 April 2009

[8] Madawala, U.K.; Thrimawithana, D.J.; , "A Bidirectional Inductive Power Interface for Electric Vehicles in V2G Systems," *Industrial Electronics, IEEE Transactions on* , vol.58, no.10, pp.4789-4796, Oct. 2011

[9] Chwei-Sen Wang; Stielau, O.H.; Covic, G.A.; , "Design considerations for a contactless electric vehicle battery charger," *Industrial Electronics, IEEE Transactions on* , vol.52, no.5, pp. 1308- 1314, Oct. 2005

[10] A. Karalis , J. D. Joannopoulos and M. Soljai "Efficient wireless non-radiative mid-range energy transfer", *Ann. Phys.*, vol. 323, no. 1, pp.34 -48 2008

[11] A. Kurs , A. Karalis , R. Moffatt , J. D. Joannopoulos , P. Fisher and M. Soljai "Wireless power transfer via strongly coupled magnetic resonances", *Sci. Exp.*, vol. 317, no. 5834, pp.83 -86 2007

[12] N. Tesla, "Apparatus for transmission of electrical energy," U.S. Patent 649, 621, dated May 15, 1900.

[13] Ho, S.L.; Junhua Wang; Fu, W.N.; Mingui Sun; , "A Comparative Study Between Novel Witricity and Traditional Inductive Magnetic Coupling in Wireless Charging," *Magnetics, IEEE Transactions on* , vol.47, no.5, pp.1522-1525, May 2011

[14] Mur-Miranda, J.O.; Fanti, G.; YifeiFeng; Omanakuttan, K.; Ongie, R.; Setjoadi, A.; Sharpe, N.; , "Wireless power transfer using weakly coupled magnetostatic resonators," *Energy Conversion Congress and Exposition (ECCE), 2010 IEEE* , vol., no., pp.4179-4186, 12-16 Sept. 2010
[15] SanghoonCheon; Yong-Hae Kim; Seung-Youl Kang; MyungLae Lee; Jong-Moo Lee; TaehyoungZyung; , "Circuit-Model-Based Analysis of a Wireless Energy-Transfer System via Coupled Magnetic Resonances," *Industrial Electronics, IEEE Transactions on* , vol.58, no.7, pp.2906-2914, July 2011
[16] Imura, T.; Hori, Y.; , "Maximizing Air Gap and Efficiency of Magnetic Resonant Coupling for Wireless Power Transfer Using Equivalent Circuit and Neumann Formula," *Industrial Electronics, IEEE Transactions on* , vol.58, no.10, pp.4746-4752, Oct. 2011
[17] Imura, T.; Okabe, H.; Uchida, T.; Hori, Y.; , "Study on open and short end helical antennas with capacitor in series of wireless power transfer using magnetic resonant couplings," *Industrial Electronics, 2009. IECON '09. 35th Annual Conference of IEEE* , vol., no., pp.3848-3853, 3-5 Nov. 2009
[18] Imura, T.; Okabe, H.; Hori, Y.; , "Basic experimental study on helical antennas of wireless power transfer for Electric Vehicles by using magnetic resonant couplings," *Vehicle Power and Propulsion Conference, 2009. VPPC '09. IEEE* , vol., no., pp.936-940, 7-10 Sept. 2009
[19] T.C.Beh, M. Kato, T. Imura, Y. Hori, "Wireless Power Transfer System via Magnetic Resonant Coupling at Fixed Resonance Frequency –Power Transfer System Based on Impedance Matching–", in *Proc. The 25th World Battery, Hybrid and Fuel Cell Electric Vehicle Symposium & Exhibition (EVS25),* 2010
[20] TeckChuanBeh; Imura, T.; Kato, M.; Hori, Y.; , "Basic study of improving efficiency of wireless power transfer via magnetic resonance coupling based on impedance matching," *Industrial Electronics (ISIE), 2010 IEEE International Symposium on* , vol., no., pp.2011-2016, 4-7 July 2010
[21] Sample, A.P.; Meyer, D.A.; Smith, J.R.; , "Analysis, Experimental Results, and Range Adaptation of Magnetically Coupled Resonators for Wireless Power Transfer," *Industrial Electronics, IEEE Transactions on* , vol.58, no.2, pp.544-554, Feb. 2011
[22] Thuc Phi Duong; Jong-Wook Lee; , "Experimental Results of High-Efficiency Resonant Coupling Wireless Power Transfer Using a Variable Coupling Method," *Microwave and Wireless Components Letters, IEEE* , vol.21, no.8, pp.442-444, Aug. 2011
[23] Awai, I.; Komori, T.; , "A Simple and versatile design method of resonator-coupled wireless power transfer system," *Communications, Circuits and Systems (ICCCAS), 2010 International Conference on* , vol., no., pp.616-620, 28-30 July 2010
[24] TakehiroImura, Toshiyuki Uchida, Yoichi Hori, "Flexibility of Contactless Power Transfer using MagneticResonance Coupling to Air Gap and Misalignment for EV", *World Electric Vehicle Association Journal,*Vol.3, 2010
[25] van Bezooijen, A.; de Jongh, M.A.; van Straten, F.; Mahmoudi, R.; van Roermund, A.; , "Adaptive Impedance-Matching Techniques for Controlling L Networks," *Circuits and Systems I: Regular Papers, IEEE Transactions on* , vol.57, no.2, pp.495-505, Feb. 2010
[26] Arroyo-Huerta, E.; Diaz-Mendez, A.; Ramirez-Cortes, J.M.; Garcia, J.C.S.; , "An adaptive impedance matching approach based on fuzzy control," *Circuits and Systems, 2009. MWSCAS '09. 52nd IEEE International Midwest Symposium on* , vol., no., pp.889-892, 2-5 Aug. 2009
[27] Hirose, Y.; Kawamura, A.; Takayanagi, A.; Takada, H.; , "Analysis of impedance matching control," *Power Electronics and Motion Control Conference, 2009. IPEMC '09. IEEE 6th International* , vol., no., pp.1188-1191, 17-20 May 2009
[28] Cao-Minh Ta; Hori, Y.;, "Convergence improvement of efficiency-optimization control of induction motor drives," *Industry Applications, IEEE Transactions on* , vol.37, no.6, pp.1746-1753, Nov/Dec 2001

TeckChuan Beh(S'09) received his B.E. degree in electrical engineering from the University of Tokyo, Japan in March 2010, and M.S. degree in advanced energy engineering from the Graduate School of Frontier Science in the same university. He is currently working in GE Healthcare Japan as an engineer. His research interests are wireless power transfer, circuit design, power electronics and medical devices.

Masaki Kato received the B.E. degree in electrical engineering from Shibaura Institute of Technology, Tokyo and the M.S degree in advanced energy engineering from the Graduate School of Frontier Science, University of Tokyo, Japan. He used to work for Honda Elesys Co., Ltd, and is currently pursuing the Ph.D at the University of Tokyo.

Takehiro Imura (S'09-M'10) received the B.S. degrees in electrical and electronics engineering from Sophia University, Tokyo, Japan. He received the M.S degree and Ph.D in Electronic Engineering from the University of Tokyo in March 2007 and March 2010 respectively. He is currently a research associate in the Graduate School of Frontier Sciences in the same university. He is now researching the wireless power transfer for EVs using electromagnetic resonant couplings.

Sehoon Oh (S'05-M'06) received the B.S., M.S., and Ph.D. degrees in electrical engineering from The University of Tokyo, Tokyo, Japan, in 1998, 2000, and 2005, respectively.
After his career as a research professor in the Department of Electrical Engineering, The University of Tokyo, he is now a senior engineer at Samsung Heavy Industries. His research fields include the development of human-friendly motion control algorithms and assistive devices for people. Dr. Oh is a member of the Institute of Electrical Engineers of Japan.

Yoichi Hori (S'81-M'83-SM'00-F'05) received his B.S., M.S., and Ph.D. degrees in Electrical Engineering from the University of Tokyo, Tokyo, Japan, in 1978, 1980, and 1983, respectively. In 1983, he joined the Department of Electrical Engineering, The University of Tokyo, as a Research Associate. He later became an Assistant Professor, an Associate Professor, and, in 2000, a Professor at the same university. In 2002, he moved to the Institute of Industrial Science as a Professor in the Information and System Division, and in 2008, to the Department of Advanced Energy, Graduate School of Frontier Sciences, the University of Tokyo. From 1991-1992, he was a Visiting Researcher at the University of California at Berkeley.
His research fields are control theory and its industrial applications to motion control, mechatronics, robotics, electric vehicles, etc. Prof. Hori has been the Treasurer of the IEEE Japan Council and Tokyo Section since 2001. He is the winner of the Best Transactions Paper Award from the IEEE Transactions on Industrial Electronics in 1993 and 2001, of the 2000 Best Transactions Paper Award from the Institute of Electrical Engineers of Japan (IEEJ), and 2011 Achievement Award of IEE-Japan. He is an IEEE Fellow and an AdCom member of IES. He is also a member of the Society of Instrument and Control Engineers; Robotics Society of Japan; Japan Society of Mechanical Engineers; and the Society of Automotive Engineers of Japan. He is the past- President of the Industry Applications Society of the IEEJ, the President of Capacitors Forum, and the Chairman of Motor Technology Symposium of Japan Management Association (JMA) and the Director on Technological Development of SAE-Japan (JSAE).